

## Effects of micronization on optical property of ceramic pigments for digital ink-jet printing

Ji-Hyeon Lee<sup>a,b</sup>, Hae-Jin Hwang<sup>b</sup>, Jong-Woo Kwon<sup>a</sup>, Jin-Ho Kim<sup>a</sup>, Kwang-Taek Hwang<sup>a</sup> and Kyu-Sung Han<sup>a,\*</sup>

<sup>a</sup>Ceramic ware Center, Korea Institute of Ceramic Engineering and Technology, Icheon 17303, Korea

<sup>b</sup>Division of Material Science and Engineering, Inha University, Incheon 22212, Korea

Digital ink-jet printing technique, which uses ceramic pigments as colorant, has been widely applied in the ceramic industry. In general, the ceramic pigments synthesized with conventional methods have particle sizes of several micrometers, and pigment particles of such sizes induce the nozzle clogging problem of print head in the ink-jet printing process. In this study, cyan, magenta, yellow, and black (CMYK) ceramic pigments were micronized to the particle sizes suitable for digital ink-jet printing through high energy milling process. The effects of micronization process on the pigment properties such as the particle morphology, crystal structure, and  $L^*a^*b^*$  color changes were investigated in detail.

**Key words:** Ink-jet printing, Ceramic pigments, CMYK, Micronization.

### Introduction

The main purpose of decoration in the ceramic products manufacturing is to increase aesthetic values. Up to now, patterns or images were printed on the product surfaces by conventional printing methods such as silk printing, gravure printing, and offset printing in order to add designs on product surfaces [1]. However, it is not easy to print various and high resolution designs with these conventional printing techniques, and there is a limitation in satisfying the demands of high quality design. Digital ink-jet printing is a technique that prints a pattern or image by sending digitalized design data from a computer to a printer and jetting ink droplets on desired positions. Digital ink-jet printing is highly efficient and environmental friendly, because ink droplets are jetted only on the desired positions and almost no waste of ink occurs [2,3]. Creation and modification of design can be easily performed with digitalized process, thus it is possible to respond effectively to rapidly changing demands for design compared to the conventional printing techniques. Based on such advantages, applications of digital printing technique in industrial fields have been spreading quickly in not only the ceramic industry but also various industrial areas in last several years [4, 5].

Ceramic pigments with excellent thermal and chemical resistance have been widely used as colorants for ceramic products, which are generally manufactured

through high temperature firing process [6, 7]. The synthesis methods of ceramic pigments include solid state reaction [8], polymerized complex method [9], and sol-gel method [10]. Among these synthesis methods, the solid state reaction is a very suitable method for mass production due to its simple and economical process. The solid state reaction is a synthesizing method using ionic or atomic diffusion, which occurs on the adjacent surfaces between particles, by forming a high temperature environment after mixing powder such as oxides or carbonates.

To apply ceramic pigments to digital ink-jet printing process, it is necessary to formulate ceramic ink which can be compatible with printer instrument. Appropriate rheological behavior and pigment particle size are required for a suitable jetting in digital ink-jet printing [11, 12]. However, the ceramic pigments synthesized by solid state method generally show particle sizes of several  $\mu\text{m}$  due to the particle growth during the high temperature synthesis process [13]. Thus, micronization process must be carried out to apply such ceramic pigments to digital printing. The micronized ceramic pigments can prevent the nozzle clogging problem of print head, and have larger surface coverage in the printing process than the ceramic pigments before micronization process [14]. According to literature, suitable ceramic particle size for ink-jet printing is known that below 300nm in average diameter or 50 times smaller  $d_{90}$  value than print head nozzle diameter [15, 16].

In this work, cyan, magenta, yellow, black (CMYK) ceramic pigments, which are four primary color in digital printing process, were micronized, and the effect of the micronization process on physical properties of

\*Corresponding author:  
Tel : +82-31-645-1404  
Fax: +82-31-645-1488  
E-mail: kh389@kicet.re.kr

CMYK ceramic pigments was investigated in detail.

## Materials and test Methods

CMYK ceramic pigments were prepared by the solid state method. The starting materials for ceramic pigment synthesis were: CoO (Sigma Aldrich, USA), Al<sub>2</sub>O<sub>3</sub> (Sumitomo, Japan) for the cyan pigment, CaO (Junsei, Japan), SnO<sub>2</sub> (Junsei, Japan), SiO<sub>2</sub> (Showa, Japan) and fluxing agents (NaX, where X = Cl, F) for the magenta ceramic pigment; ZrO<sub>2</sub> (Sigma Aldrich, USA), SiO<sub>2</sub> (Showa, Japan), Pr<sub>6</sub>O<sub>11</sub> (Sigma Aldrich, USA) and fluxing agents (NaX, where X = Cl, F) for the yellow ceramic pigment; and CoO (Sigma Aldrich, USA), Fe<sub>2</sub>O<sub>3</sub> (Junsei, Japan), and Cr<sub>2</sub>O<sub>3</sub> (Junsei, Japan) for the black ceramic pigment. The amount of starting materials needed for each ceramic pigment was adjusted according to the stoichiometric ratio, and they were mixed with alumina balls of 10 mm diameter and ethanol by milling for 3 hrs. Afterwards, the dried powders were sintered at 1,000 °C for cyan and black, 1,300 °C for magenta, and 1,100 °C for yellow for 1 hr under the oxidizing atmosphere with the heating rate of 5 °C/min.

The micronization process of ceramic pigments was carried out by using a nanoset mill (KMD-1S, DNTEK, Korea). Zirconia balls of 0.5 mm diameter were used. The distilled water, ceramic pigments, and zirconia balls were put in with the weight ratios of 6:2:1. The micronization process of ceramic pigment powder was carried out at the speed of 2,000 rpm. The micronization process was aimed at jetting from the inkjet head with a nozzle diameter of 45 μm.

The crystal structure analysis of CMYK ceramic pigments before and after micronization process was conducted by XRD (D-Max 2500, Rigaku, Japan), and the identifications of measured XRD patterns were analyzed by using an XRD analysis software (PDXL2, Rigaku, Japan). The microstructures of pigment particles were analyzed by using FE-SEM (JSM-6390, Jeol, Japan). The pigment particle size distribution and specific surface area were measured with PSA (LA-950V2, Horiba, Japan) and surface area analyzer (Tristar II, Micromeritics, USA), respectively. Furthermore, to analyze the optical property changes before and after micronization process, the CIE (Commission Internationale de l'Eclairage) color system values (*L\*a\*b\**) and the absorption spectra were measured by using a UV-visible spectrophotometer (V-770, Jasco, Japan).

## Results and Discussion

The micronization process using high-energy milling basically reduces particle size. It also affects the change in crystal structure due to the decrease in particle size. The crystal structure changes before and after micronization of synthesized CMYK ceramic pigments

are shown in Fig. 1. In the case of cyan pigment, CoAl<sub>2</sub>O<sub>4</sub>, which has a spinel structure, is shown as a main phase, and Al<sub>2</sub>O<sub>3</sub>, which seems to be an unreacted residue, is shown as a secondary phase. For the magenta pigment, CaSnO(SiO<sub>4</sub>) having a malayite structure is shown as a main phase and SiO<sub>2</sub> as secondary phase. For the yellow pigment, ZrSiO<sub>4</sub> of zircon structure is shown as a main phase and ZrO<sub>2</sub>, which seems to be an unreacted residue, is shown as secondary phase. In the case of black pigment, Co(Fe, Cr)<sub>2</sub>O<sub>4</sub> of spinel structure is shown as a main phase and CoO as secondary phase.

As the micronization was carried out for all the CMYK ceramic pigments, the full width at half maximum (FWHM) increase and the intensity decrease of XRD pattern were observed (Fig. 2(a)). According to the literatures, a peak broadening and decrease in peak intensity are the result of reduction of crystal size [17, 18]. Fig. 2(b) shows the crystal size changes of CMYK ceramic pigments calculated by using the Halder-Wagner method [19, 20]. The crystal size of CMYK ceramic pigments were declined according to micronization time. These results indicate that the high energy milling for the micronization process has not only affected the size reduction effects but also the crystal structural changes.

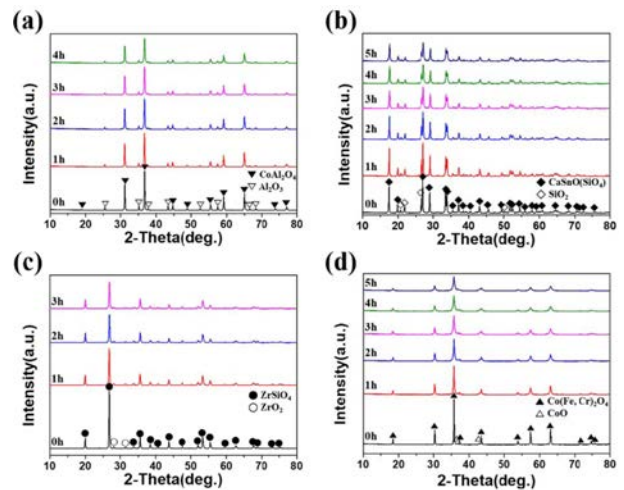


Fig. 1. XRD patterns of ceramic pigments during micronization process: (a) cyan, (b) magenta, (c) yellow and (d) black.

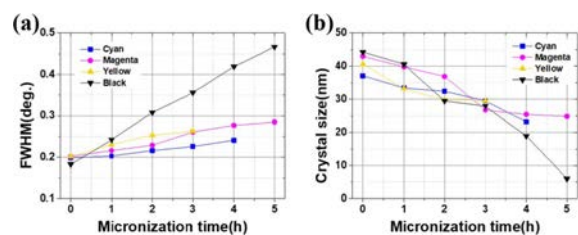
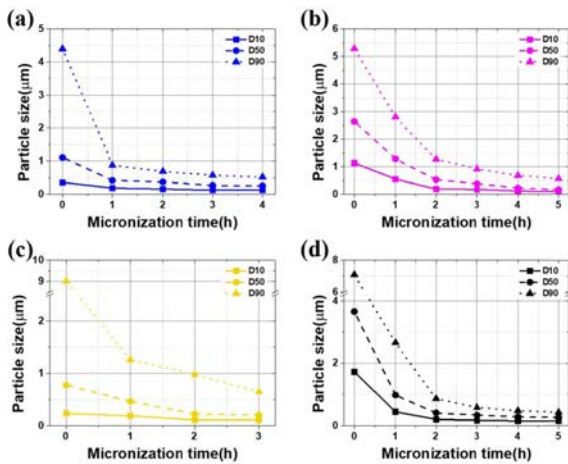
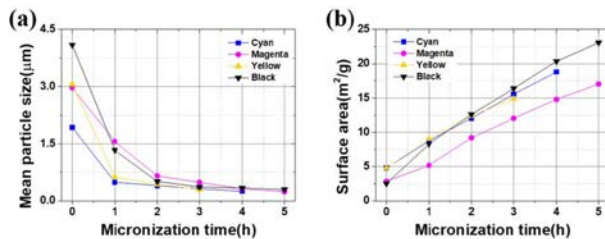


Fig. 2. (a) FWHM and (b) crystal size of CMYK ceramic pigments during micronization process.



**Fig. 3.** Particle size percentile of CMYK ceramic pigments during micronization process: (a) cyan, (b) magenta, (c) yellow and (d) black.



**Fig. 4.** (a) Mean particle size and (b) surface area of CMYK ceramic pigments during micronization process.

The micronization behavior of CMYK ceramic pigments according to the milling process was observed by using PSA of laser diffraction method. Fig. 3 shows the particle size of CMYK ceramic pigment as the 10th, 50th and 90th percentiles of the cumulative curve according to the micronization process. The particle size reduction of CMYK ceramic pigments tended to decrease rapidly until the critical micronization time was reached, rather than linearly. After critical micronization time, no large size reduction was observed. The critical micronization time for each color of the pigments were 1 hr cyan and yellow, and 2 hrs for magenta and black, respectively. The D90 value of CMYK ceramic pigments after micronization process showed 50 times smaller than aimed print head nozzle diameter of 45  $\mu\text{m}$ . Thus, nozzle clogging is not expected.

In Fig. 4(a), the average particle size changes of CMYK ceramic pigments are shown according to the micronization time. The average particle size of cyan pigment showed a large change from 1.9  $\mu\text{m}$  to 489.0 nm after 1 hr of micronization. Afterwards, the change of particle size according to the micronization time slowed down, and after 4 hours of micronization, it reached 251.2 nm. In the case of magenta ceramic pigment, the average particle size decreased greatly

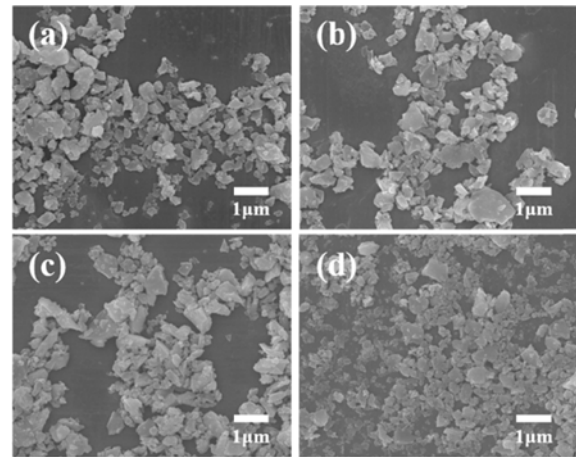


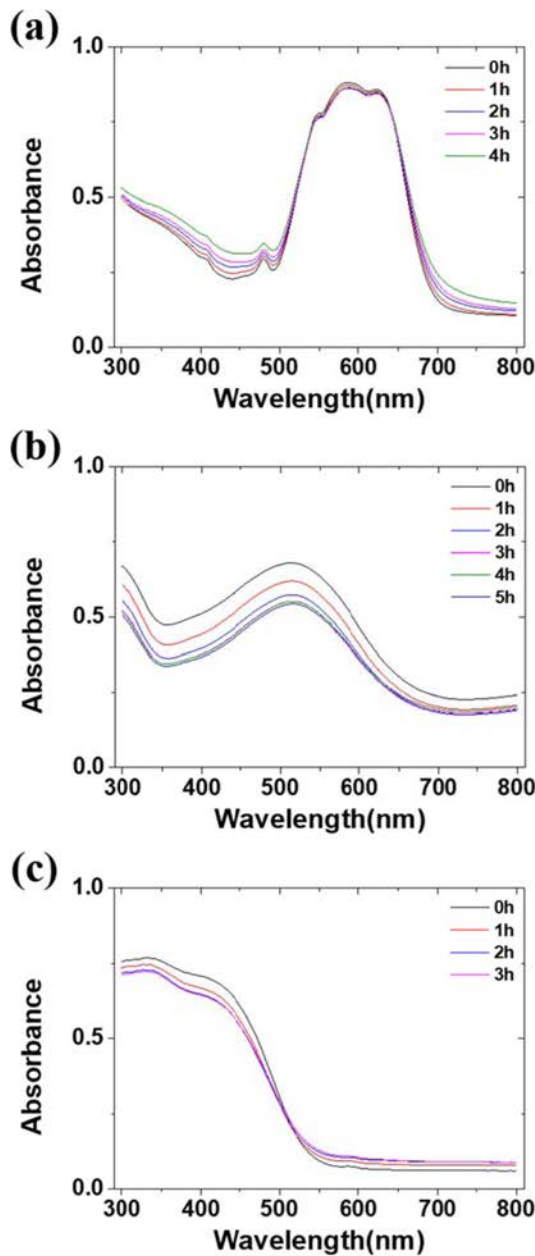
**Fig. 5.** FE-SEM images of ceramic pigments after micronization process: (a) cyan, (b) magenta, (c) yellow and (d) black.

from 3.0  $\mu\text{m}$  to 656.2 nm after 2 hrs of micronization. Afterwards, the average particle size changes showed a slowing down trend, and 5 hours after micronization, it reached 241.0 nm. The yellow ceramic pigment showed the average particle size of 3.1  $\mu\text{m}$ , which was decreased sharply to 630.1 nm after 1 hr of micronization. The average particle size was 298.1 nm after 3 hours of micronization. The black ceramic pigment initially showed the average particle size of 2.9  $\mu\text{m}$  before micronization, and the average particle size reached 299.3 nm after 5 hrs of micronization.

Fig. 4(b) shows the specific surface area of CMYK ceramic pigments according to the micronization process. The specific surface area of CMYK ceramic pigments were gradually increased. It was determined that these results occurred because new interfaces of ceramic pigments were continuously produced as the micronization process was carried out.

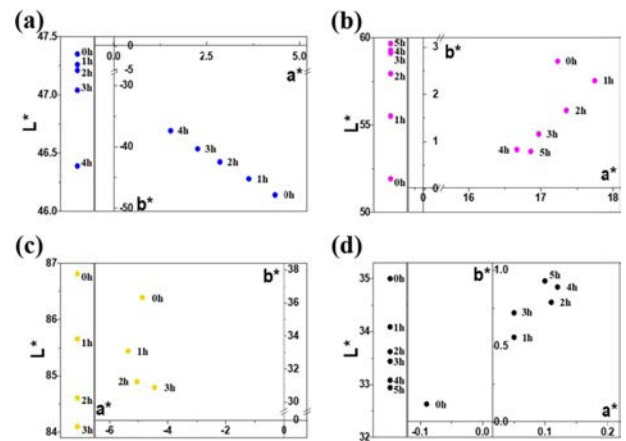
Fig. 5 shows the morphologies of CMYK ceramic pigments after micronization. Most particles of CMYK ceramic pigments had the particle sizes of less than 900 nm after the micronization. It was observed that the pigment particles were broken down into fine particles by high mechanical energy, resulting irregular particle shapes. A common characteristic of micronized CMYK ceramic pigments was that it consists mainly of fragments with rough edges. The pigment with this morphology affects viscosity property at the ceramic ink synthesis process [21].

Fig. 6 shows the absorption spectra for the cyan, magenta, and yellow pigments. The black ceramic pigment was excluded from the analysis, because it absorbs almost all wavelengths in the visible light region [22]. The crystal structure of the pigment is composed of transition metals and ligands which coordinating transition metal. In this structure, orbital energy splitting is occurred due to an interaction



**Fig. 6.** Absorption spectra of ceramic pigments during micronization process: (a) cyan, (b) magenta, (c) yellow.

between transition metal and ligand. The orbital energy splitting can be indicated as an energy level and particular wavelength, which corresponding to energy level, is absorbed. Consequently, this phenomenon leads color difference of pigments [23, 24]. The cyan ceramic pigment showed a strong absorption band at 585 nm, which corresponded to the orange wavelength region, and this result was shown in Fig. 6(a). Such absorption spectra of cyan ceramic pigment were resulted because the d-d transition of  $\text{Co}^{2+}$  ions located in the tetrahedral coordination of spinel structure occurred from the ground state  ${}^4\text{A}_2({}^4\text{F})$  to the excited



**Fig. 7.** CIE  $L^*a^*b^*$  colorimetric coordinates of ceramic pigments during micronization process: (a) cyan, (b) magenta, (c) yellow and (d) black.

state  ${}^4\text{T}_1({}^4\text{P})$  [25]. In Fig. 6(b), the magenta ceramic pigment shows a strong absorption band appeared at 515 nm, which corresponded to the green wavelength region. Such absorption spectra are the result appearing when the d-d transition of  $\text{Cr}^{4+}$  ions located in the octahedral coordination of malayite structure occurs from the ground state  ${}^3\text{T}_1({}^3\text{F})$  to the excited state  ${}^3\text{T}_2({}^3\text{F})$  [26]. In Fig 6(c), the yellow ceramic pigment shows a strong absorption band was shown at 335 nm, which was in the ultraviolet wavelength region, and it seemed to be because the f-d transition of  $\text{Pr}^{4+}$  ions occurred from the ground state  $2t_{2g}$  to the excited state f. A strong absorption band was also shown at 410 nm, which was in the visible light wavelength region, and it was because for this absorption band, the f-f transition of  $\text{Pr}^{4+}$  ions occurred from the ground state  $t_{1g}$  to the excited state f [27, 28]. Lastly, a weak absorption band appeared at 590 nm because the f-f transition of  $\text{Pr}^{3+}$  ions occurred from the ground state  ${}^3\text{H}_4$  to the excited state  ${}^1\text{D}_2$  [29, 30].

The decreases of particle size due to the micronization affect the scattering and absorption of wavelengths incident on the pigments, thereby changing the optical properties [31]. To confirm the color changes according to the milling process, Fig. 7 shows the  $L^*a^*b^*$  measurement values before and after micronization of CMYK ceramic pigments. In the CIE  $L^*a^*b^*$  color space,  $L^*$  value means the lightness, and 0 indicates black and as it gets closer to 100, it becomes whiter.  $a^*$  shows which side the color is leaning toward between red and green; if  $a^*$  is negative (-), it indicates green and if positive (+), red. In the case of  $b^*$ , if negative (-), it indicates blue and if positive (+), yellow.

The  $L^*$  and  $a^*$  value of cyan ceramic pigment was slightly decreased after micronization process. Whereas  $b^*$  value tended to increase. From these results, cyan ceramic pigment showed a decrease in brightness and blue tone after micronization. Such a blue tone



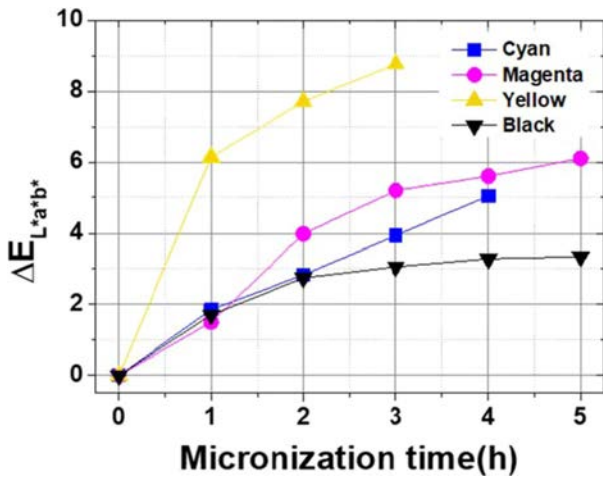


**Fig. 8.** Total color difference of ceramic pigments during micronization process: (a) cyan, (b) magenta, (c) yellow and (d) black.

reduction seems to be related to the decrease of characteristic absorption spectra of cyan ceramic pigment corresponding to 585 nm in Fig. 6(a).  $L^*$  value of magenta ceramic pigment was increased after micronization process. On the other hands,  $a^*$  and  $b^*$  values indicated a decrease. The result of this color change was an effect of decrease of characteristic absorption spectra corresponding to 515 nm of Fig. 6(b). After micronization, The  $L^*$  and  $a^*$  values were decreased. Whereas insignificant change of  $b^*$  values was observed. Because of micronization, decreased brightness of yellow pigment and yellow tone was shown. It was determined that the change of yellow tone in the yellow ceramic pigment was due to the decrease of characteristic absorption spectra corresponding to 410 nm shown in Fig. 6(c). Lastly, The  $L^*$  value of black

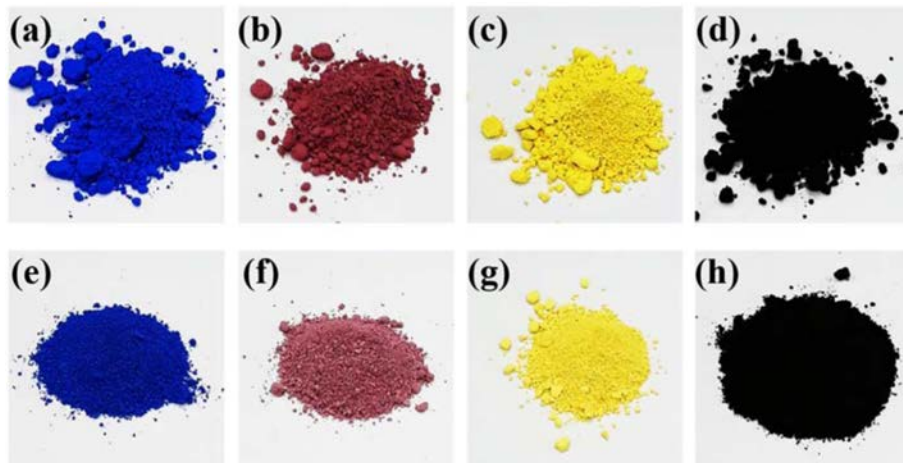
ceramic pigment was declined after micronization. On the contrary, significant color changes were not observed in  $a^*$  and  $b^*$  values. According to the micronization time, brightness of the black ceramic pigment decreased, but the chroma changed insignificantly.

Fig. 8 and Fig. 9 show the color changes of CMYK ceramic pigments according to the micronization time. value shows the total color difference of CMYK ceramic pigments before and after micronization, and it was calculated by using the following equation:

$$\Delta E_{L^*a^*b^*} = [(\Delta L^*)^2 + (\Delta a^*)^2 + (\Delta b^*)^2]^{1/2} \quad (1)$$

$\Delta L^*$ ,  $\Delta a^*$ , and  $\Delta b^*$  values show the changes of  $L^*$ ,  $a^*$ , and  $b^*$ , respectively, before and after micronization [32].  $\Delta E_{L^*a^*b^*}$  value of all ceramic pigments used in the experiment showed an increasing trend as the micronization time passed. The total color difference shown in the present experiment can be regarded as the color deterioration level of CMYK ceramic pigments.  $\Delta E_{L^*a^*b^*}$  value after completion of micronization was 10.9 for the cyan, 8.0 for the magenta, 6.1 for the yellow, and 2.2 for the black. Among the CMYK ceramic pigments, the cyan showed the largest color change whereas the black showed the smallest change. In the results shown for the present experiment, the decreasing phenomenon of crystal size and particle size and deterioration phenomenon of color occurred simultaneously. Therefore, it can be concluded that the crystal structure changes of ceramic pigments due to micronization led to the color deteriorations.

Inkjet printing ink with ceramic pigments is mainly used for decoration of ceramic objects. Due to the printing process of ceramic objects normally undergo heat treatment above 1000 °C, the printed ceramic pigments must not change color after heat treatment process. Fig. 10 showed the results of heat treatments



**Fig. 9.** Photo images of ceramic pigments before micronization: (a) cyan, (b) magenta, (c) yellow, (d) black and after micronization: (e) cyan, (f) magenta, (g) yellow, (h) black.

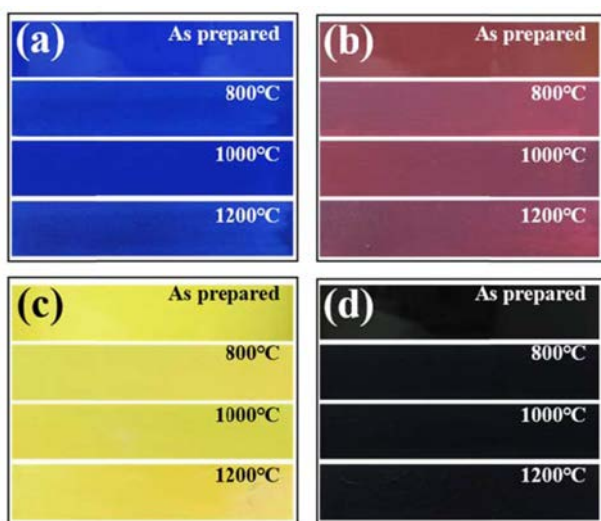


**Fig. 10.** Thermal stability of micronized ceramic pigments at various heat treatment temperatures: (a) cyan, (b) magenta, (c) yellow and (d) black.

of the micronized CMYK ceramic pigments at 800 °C, 1000 °C and 1200 °C respectively. CMYK ceramic pigments showed stable color performance after heat treatment at 800 °C and 1000 °C, and even at the heat treatment temperature of 1200 °C, which is higher than the cyan, yellow, black ceramic pigment synthesis temperature.

## Conclusions

The effects of micronization process on the physical properties of CMYK ceramic pigments, which are four primary colors in digital printing, were investigated to apply the CMYK ceramic pigments to digital printing. The synthesized CMYK ceramic pigments were successfully micronized from several  $\mu\text{m}$  to less than 300nm, which is required for ink-jet printing. The optical properties of CMYK ceramic pigments were well maintained after micronization process with high thermal stability at over 1000 °C.

## Acknowledgements

This work was supported from the R&D program (KPP170002, Development of Functional Ceramic Tile using Surface Glaze Modification) by Korea Institute of Ceramic Engineering and Technology.

## References

1. V.S. Solana, Qualicer (2014) 1-15.
2. S. Magdassi, in "The Chemistry of Inkjet Inks" (World Scientific Publishing Co., 2009) p. 5.
3. I. Hutchings, Actas de QUALICER (2010) 1-16.
4. G. P. Crasta, Ceramic World Review 97 (2012) 64-88.
5. G. Savvidis, M. Zarkogianni, E. Karanikas, N. Lazaridis, N. Nikolaidis and E. Tsatsaroni, Color. Technol. 129 (2012) 55-63.
6. M. Dondi, Appl. Clay Sci. 15 (1999) 337-366.
7. F. Bondioli, F. Andreola, L. Barbieri, T. Manfredini and A.M. Ferrari, J. Eur. Ceram. Soc. 27 (2007) 3483-3488.
8. G. George, L.S. Kumari, V.S. Vishnu, S. Ananthakumar and M.L.P. Reddy, J. Solid State Chem. 181 (2008) 487-492.
9. S. A. Eliziário, J.M.D. Andrade, S.J.G. Lima, C.A. Paskocimas, L.E.B. Soledade, P. Hammer, E. Longo, A.G. Souza and I.M.G. Santos, Mater. Chem. Phys. 129 (2011) 619-624.
10. M.A. Tena, A. Mestre, A. Garcí'a, S. Sorli' and G. Monro's, J. Sol-Gel Sci. Technol. 26 (2003) 813-816.
11. D. Kuscer, G. Stavber, G. Trefalt and M. Kosec, J. Am. Ceram. Soc. 95 [2] (2012) 487-493.
12. M. Dondi, M. Blosi, D. Gardini and C. Zanelli, Ceram Forum Int. 89 (2012) 59-64.
13. D. Guo, Q. Yang., P. Chen, Y. Chu, Y Zhang and P. Rao, Dyes Pigm. 153 (2018) 74-83.
14. C. Zanelli, G. L. Güngör, A. Kara, M. Blosi, D. Gardini, G. Guarini and M. Dondi, Ceram. Int. 41 (2015) 6507-6517.
15. M. Dondi, M. Blosi, D. Gardini, C. Zanelli, Qualicer 2012-XII Global Forum on Ceramic Tile (2012) 1-12.
16. D. Kuscer, G. Stavber, G. Trefalt and M. Kosec, J. Am. Ceram. Soc. 95[2] (2012) 487-493.
17. T. Ungár, Scripta Mater. 51[8] (2004) 777-781.
18. R. Yogamalar, R. Srinivasan, A. Vinu, K. Ariga and A.C. Bose, Solid State Commun. 149[43] (2009) 1919-1923.
19. N.C. Halder and C.N.J. Wagner, Acta. Cryst. 20 (1966) 312-313.
20. N.C. Halder and C.N.J. Wagner, Adv. X-Ray Anal. 9 (1966) 91-102.
21. D. Gardini, M. Blosi, C. Zanelli and M. Dondi, J. Nanosci. Nanotechnol. 15 (2015) 3552-3561.
22. W. Wang, W. Liu, X. Yang, and Z. Xie, Ceram. Int. 38 (2012) 2851-2856.
23. S. Tamilarasan, S. Laha, S. Natarajan and J. Gopalakrishnan, Eur. J. Inorg. Chem. (2016) 288-293.
24. A.S. Marfunin, in "Physics of Minerals and Inorganic Materials" (Springer Berlin Heidelberg, 1979).
25. X. Duan, M. Pan, F. Yu and D. Yuan, J. Alloys Compd. 509 (2011) 1079-1083.
26. A.M. Heyns and P.M. Harden, J. Phys. Solids 60 (1999) 277-284.
27. H.E. Hoefdraad, J. Inor. Nucl. Chem. 37 [3] (1975) 1917-1921.
28. D. Pawlak, Z. Frukacz, Z. Mierczyk, A. Suchocki, and J. Zachara, J. Alloy. Comp. 275[2] (1998) 361-364.
29. G. De, A. Licciulli and M. Nacucchi, J. Non-Crys. Solid 201[1] (1996) 153-58.
30. H. Friis, A.A. Finch, C.T. Williams and J.M. Hanchar, Phys. Chem. Minerals. 37 (2010) 333-342.
31. G. Buxbaum, in "Industrial Inorganic Pigments, second ed." (Wiley-VCH, 1998) p. 289.
32. R. S. Berns, in "Billmeyer and Saltzman's Principles of Color Technology" (John Wiley & Sons, 2000) p. 72.